NeuroImage 190 (2019) 46–55

Contents lists available at ScienceDirect

NeuroImage

journal homepage: www.elsevier.com/locate/neuroimage

Preserved canonicality of the BOLD hemodynamic response reflects healthy cognition: Insights into the healthy brain through the window of Multiple Sclerosis

Monroe P. Turner [a], Nicholas A. Hubbard [b], Dinesh K. Sivakolundu [a], Lyndahl M. Himes [a], Joanna L. Hutchison [a], John Hart Jr. [a,c], Jeffrey S. Spence [a], Elliot M. Frohman [c], Teresa C. Frohman [c], Darin T. Okuda [c], Bart Rypma [a,d,*]

[a] School of Behavioral and Brain Sciences, University of Texas at Dallas, Richardson, TX, USA
[b] McGovern Institute for Brain Research, Massachusetts Institute of Technology, Cambridge, MA, USA
[c] Department of Neurology, University of Texas Southwestern Medical Center, Dallas, TX, USA
[d] Department of Psychiatry, University of Texas Southwestern Medical Center, Dallas, TX, USA

A B S T R A C T

The hemodynamic response function (HRF), a model of brain blood-flow changes in response to neural activity, reflects communication between neurons and the vasculature that supplies these neurons in part by means of glial cell intermediaries (e.g., astrocytes). Intact neural-vascular communication might play a central role in optimal cognitive performance. This hypothesis can be tested by comparing healthy individuals to those with known white-matter damage and impaired performance, as seen in Multiple Sclerosis (MS). Glial cell intermediaries facilitate the ability of neurons to adequately convey metabolic needs to cerebral vasculature for sufficient oxygen and nutrient perfusion. In this study, we isolated measurements of the HRF that could quantify the extent to which white-matter affects neural-vascular coupling and cognitive performance. HRFs were modeled from multiple brain regions during multiple cognitive tasks using piecewise cubic spline functions, an approach that minimized assumptions regarding HRF shape that may not be valid for diseased populations, and were characterized using two shape metrics (peak amplitude and time-to-peak). Peak amplitude was reduced, and time-to-peak was longer, in MS patients relative to healthy controls. Faster time-to-peak was predicted by faster reaction time, suggesting an important role for vasodilatory speed in the physiology underlying processing speed. These results support the hypothesis that intact neural-glial-vascular communication underlies optimal neural and cognitive functioning.

Introduction

The hemodynamic response function (HRF) models the time course of the change in blood flow in response to a brief change in neural activity that is measured with functional magnetic resonance imaging (fMRI; Kwong et al., 1992; Ogawa et al., 1990, 1992). As such, in the healthy system, it is generally considered to be a proxy for underlying neural activity originating in gray-matter. It is known to result from a complex interplay of neurons, glial cell intermediaries (e.g., astrocytes), and blood vessels that together constitute the mechanism by which neurons communicate their metabolic needs to blood vessels, and by which blood vessels return oxygen and metabolites to neurons (e.g., Attwell et al., 2010; Cauli and Hamel, 2010; Iadecola, 2017; Lundgaard et al., 2014; Metea and Newman, 2006; Rossi, 2006; Takano et al., 2006). Thus, in healthy young adults, the HRF actually indexes regional displacement of metabolically generated deoxyhemoglobin by the flow of oxyhemoglobin following neural activity in the form of the blood-oxygen-level-dependent (BOLD) signal.

Due to the reliability of the HRF, it assumes a canonical shape in young healthy individuals (see Fig. 1). Thus, most fMRI studies utilize a canonical HRF in analysis (see Lindquist et al., 2009). However, it is known to vary considerably in aging and disease (e.g., Bonakdarpour et al., 2007; D'Esposito et al., 1999; D'Esposito et al., 2003; Hubbard et al., 2016a; Rypma & D'Esposito, 2001; Zou et al., 2011). Because of the reliance upon neural-vascular communication to produce this canonical shape (e.g., Buxton et al., 2004; Martin et al., 2006), comparisons between healthy individuals and those with known neural-vascular coupling compromise would permit testing of hypotheses regarding the importance of an intact neural-vascular coupling system to optimal neural and cognitive performance.

In Multiple Sclerosis (MS), the integrity of the glial cell intermediaries known to facilitate neural-vascular communication is damaged (De

* Corresponding author. School of Behavioral and Brain Sciences, Center for Brain Health, University of Texas at Dallas, 800 West Campbell Road, Richardson, TX, 75080, USA.
E-mail address: bart.rypma@utdallas.edu (B. Rypma).

https://doi.org/10.1016/j.neuroimage.2017.12.081
Received 2 June 2017; Received in revised form 18 December 2017; Accepted 22 December 2017
Available online 15 February 2018
1053-8119/

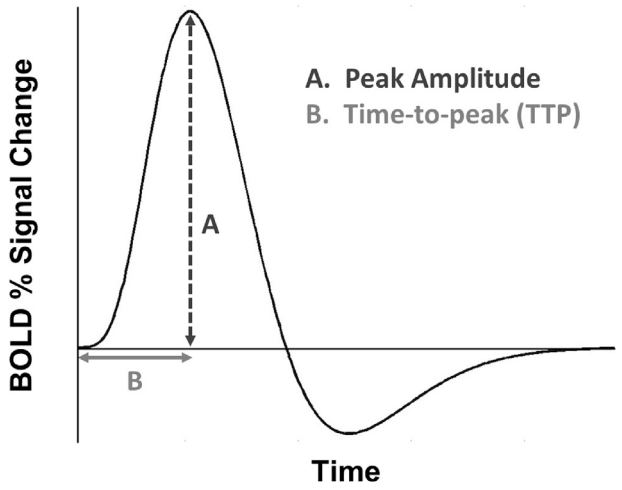

Fig. 1. Canonical hemodynamic response function (HRF), a model of the change in blood-oxygen-level-dependent signal through time.

Keyser et al., 2008; D'Haeseleer et al., 2011; Gareau et al., 1999; Jukkola et al., 2013; Lassmann, 2003, 2014; Lundgaard et al., 2014; Mulligan and MacVicar, 2004; Petzold and Murthy, 2011; Trapp and Nave, 2008; Trapp and Stys, 2009). One potential consequence of this damage is a compromised ability of neurons to convey their metabolic needs to vasculature, resulting in insufficient oxygen and nutrient perfusion (see De Keyser et al., 2008; Debernard et al., 2013; D'Haeseleer et al., 2011). Because reduced white-matter integrity in MS probably disrupts neural-vascular communicating structures, comparisons to healthy individuals can elucidate the roles of these structures in the healthy brain, including in neural-vascular coupling.

Ascertaining the best model of the HRF for group comparisons has been debated in fMRI literature. Several studies have provided evidence for the appropriateness of gamma functions (e.g., Friston et al., 1998; Maus et al., 2012; cf. Lindquist and Wager, 2007; Lindquist et al., 2009). However, these models rely on the validity of group-equivalence assumptions regarding HRF shape (e.g., that maximum BOLD signal occurs at a fixed time point after stimulus onset; but see Henson et al., 2002). Neurocognitive aging research, for instance, has demonstrated the consequences of HRF between-groups equivalence assumptions, yielding both false positives and false negatives (Ances et al., 2009; Hutchison et al., 2013a,b; Lindquist et al., 2009; Mohtasib et al., 2012; Pasley et al., 2007; Restom et al., 2007; cf. Aizenstein et al., 2004; Buckner et al., 2006; D'Esposito et al., 1999; Huettel et al., 2001). Canonical HRF modeling may not be any more appropriate in MS-healthy comparisons than in young-old comparisons. Greater variation in underlying hemodynamic systems seen in groups such as older adults (Hutchison et al., 2013a,b; Tsvetanov et al., 2015) and MS patients (DeLuca et al., 2008; Pantano et al., 2005; Rocca et al., 2002; Wegner et al., 2008; cf. Genova et al., 2009; Hubbard et al., 2016a; Lee et al., 2000; White et al., 2009) challenges the assumptions necessary for use of canonical HRFs in group comparison studies. In this way, HRFs derived from the use of a canonical function could be biased in their characterization of the BOLD signal response (cf. Calhoun et al., 2004; Handwerker, Ollinger, & D'Esposito, 2004).

Such bias could underlie the diversity of results that have been observed in BOLD-fMRI of MS. Some studies have observed MS-related BOLD signal increases in motor cortex during finger tapping (e.g., Pantano et al., 2005; Rocca et al., 2002; Wegner et al., 2008) and in prefrontal cortex during a processing speed task (e.g., DeLuca et al., 2008), while others have observed MS-related decreases in motor cortex BOLD signal during finger tapping (e.g., Hubbard et al., 2016a; Lee et al., 2000; White et al., 2009) and in prefrontal cortex during a processing speed task (e.g., Genova et al., 2009). Increases in BOLD signal have been suggested to reflect adaptive reorganization (e.g., Bonnet et al., 2010; Kern et al., 2012), but the underlying mechanisms remain poorly understood.

One solution to this problem involves HRF modeling techniques that minimize shape assumptions, such as spline interpolation (Carew et al., 2003; Gibbons et al., 2004; see also Glover, 1999; Goutte et al., 2000; Wink et al., 2008). Instead of fitting a single pre-conceived function to measured data points by minimizing squared error, the spline interpolation method used in this study modulates the shape of a set of (polynomial) basis functions to smoothly connect the measured data points (called knots) in piecewise fashion with the overall curvature of the entire set of functions minimized (Ramsay, 2006).

MS-related damage to white-matter structures might cause neural dysconnectivity and vascular change (Bonzano et al., 2009; Dineen et al., 2009). Law and colleagues (2004), for instance, showed reduced cerebral blood flow and prolonged transit time in MS patients' white-matter. Inability of astrocytes to mediate vasodilation in MS leads to neural-vascular communication deficits in and around active transient lesions (Carmignoto and Gómez-Gonzalo, 2010; De Keyser et al., 2008; Metea and Newman, 2006). Blood flow changes at transient-lesion sites persist after exacerbation resolution (Ge et al., 2005; Haselhorst et al., 2000). Thus, transient lesions leave in their wake white-matter dysfunction, resulting in disruption of cortical transmission necessary for efficient cognition, vascular-dependent cell metabolism, and the magnetic signature vital to fMRI known as the BOLD signal.

Cerebral vascular dynamics are known to be altered in MS (Brooks et al., 1984; Lycke et al., 1993; Mulholland et al., 2017; Rashid et al., 2004; Sun et al., 1998; Swank et al., 1983). However, based on what is known about MS neuropathology, these dynamics probably reflect microstructural damage to glial cell intermediaries in white (i.e., fibrous astrocytes) and gray matter (i.e., protoplasmic astrocytes). Global reductions in perfusion of oxygen and metabolites (De Keyser et al., 2008; Debernard et al., 2013) probably result from astrocyte dysfunction (e.g., Blanco et al., 2008; Brosnan and Raine, 2013; De Keyser et al., 1999; D'Haeseleer et al., 2011; Takano et al., 2006). One study (Marshall et al., 2014) has shown MS-related cerebrovascular reactivity reductions, but this phenomenon probably results from chronic vasodilation secondary to elevated nitric oxide concentration in cerebral tissue (e.g., Brown, 2007, 2010; Brown and Bal-Price, 2003; Brown and Borutaite, 2002; Su et al., 2009).

Optimal cognitive performance could depend on the integrity of the neural-glial-vascular system. Studies employing increased oxygen availability (i.e., hyperoxia) have demonstrated that increases in perfusion (mediated by intact neural-glial-vascular function) are associated with decreases in neural activity (Xu et al., 2012) and improvements in cognitive performance (Chung et al., 2006). Such relationships implicate neural efficiency as a mechanism underlying processing speed, the speed with which an individual can execute elementary cognitive operations (Rypma et al., 2006; Salthouse, 1992). Cognitive slowing is the most commonly observed neuropsychological deficit in MS patients, and is primarily indexed by processing speed measures such as the Digit Symbol Substitution Task (DSST; Strober et al., 2014). Variation in this basic ability is thought to mediate higher-order cognitive functions (e.g., working memory and reasoning; Ackerman et al., 2002; Rypma et al., 2006; Rypma & D'Esposito, 1999; Rypma and Prabhakaran, 2009; Salthouse, 1996; Vernon, 1983). Thus, comparisons between MS patients and healthy controls could elucidate the role of neural-glial-vascular function in processing speed.

In this study, we utilized a modeling approach not dependent on the validity of shape assumptions to quantify differences between a healthy group and one with known neural-vascular compromise that probably affects the canonical shape of their HRF (i.e., MS patients; Hubbard et al., 2016a). Thus, we tested two hypotheses. The first was that HRF shape metrics (as measured by peak amplitude and time-to-peak) will differ between MS patients and controls. The second was that these HRF shape metrics will be more associated with processing speed in MS patients

than in controls. On one hand, the finding that multiple HRF metrics account for variance in task performance would indicate widespread disruption of the neural-glial-vascular system. The finding of a single HRF metric accounting for this variance, on the other hand, would isolate a relationship between a specific component of the neural-glial-vascular system and cognition. Our findings suggest that the canonicality of the HRF indexes the health of the neural-glial-vascular system necessary for optimal cognitive performance. Thus, a canonical HRF reflects a healthy neural-vascular coupling system, critical to supporting neural function. Deviations from canonicality, and their relationships to performance, may index the extent to which the integrity of this system is compromised.

Methods

Participants

A total of 55 participants were enrolled in this study. Twenty-five healthy controls were recruited from the greater Dallas-Fort Worth Metroplex, and thirty relapsing-remitting MS patients were recruited from the University of Texas Southwestern Medical Center (UTSW) Clinical Center for Multiple Sclerosis. All participants provided informed written consent prior to scanning, and all were compensated financially for their participation. Procedures were jointly approved by Institutional Review Boards of both UTD and UTSW.

Participant recruitment was designed to age- and sex-match controls to patients, and neither attribute was significantly different between groups (see Table 1). All participants had normal or corrected-to-normal vision (one patient did report a previous history of optic neuritis, but vision was normal at scan time). Patients had neither experienced an exacerbation nor had been treated with corticosteroids for at least one month prior to scanning. Eighty-two percent of patients indicated a history of immunomodulatory therapy (i.e., interferon beta, glatiramer acetate, and/or natalizumab). Average time from initial diagnosis for MS patients was 153.19 months ($SEM = 14.72$; $n = 27$). Several participants were excluded for the following reasons: use of a psychostimulant prior to the fMRI scan (one MS patient), history of taking medication for seizures (one healthy control), and a failure to align functional MRI data with a standardized brain template (one healthy control, one MS patient; see section 2.4). Data analysis was then possible for the remaining 51 participants ($n_{Patient} = 28$; $n_{Control} = 23$).

Experimental paradigm

Participants underwent fMRI scanning during performance of two tasks. The first was a simple and commonly-employed sensorimotor button-press task (BPT). An event-related, fixed-paced experimental design was used to minimize the effects of differences in RT between groups on the HRF. Stimuli presentations were broken up by jittered rest periods of durations of 14 ± 1 s, in which a white fixation cross was displayed on-screen. In this event-related paradigm, participants were instructed to press thumb-buttons bilaterally and simultaneously as rapidly as possible after onset of a radial black-and-white checkerboard flickering at 6 Hz for 500 ms. There were 20 trials in total.

The second task involved a version of the Digit Symbol Substitution Task (DSST), modified for use in the fMRI environment (Rypma et al., 2006). In each trial, participants viewed a key of nine digit-symbol pairs and one probe digit-symbol pair for 4000 ms (see Fig. 2). Participants were asked to indicate as quickly and accurately as possible via left- or right-thumb button-press whether the probe digit-symbol pair matched one of the digit-symbol pairs in the key. Inter-trial intervals were jittered at 0, 2, 4, and 6 s intervals. Accuracy and reaction time (RT) were recorded. RT was calculated for both groups only for correct responses. Further, as a measure of external validity, we examined processing speed performance outside of the fMRI environment. There were 225 total trials across three runs (75 trials per run).

After scanning, participants completed a battery of neuropsychometric tests outside the scanner environment to characterize the samples. This battery included the Symbol Digit Modalities Test (SDMT) from the Wechsler Adult Intelligence Scale, Third Edition (WAIS-III; Wechsler, 1997), the Paced Auditory Serial Addition Task (PASAT; Gronwall, 1977), Trail Making Tests A & B (Tombaugh et al., 1998), and a box completion task (Salthouse, 1996). MS patients also completed several assessments commonly administered in MS research, including the Modified Fatigue Impact Scale (MFIS; Fisk et al., 1994) and the Expanded Disability Status Scale (EDSS; Bowen et al., 2001).

Scanning parameters

Neuroimaging data were collected at the UTSW Advanced Imaging Research Center using a Philips 3 Tesla MRI scanner (Philips Medical Systems, Best, The Netherlands) with an 8-channel SENSE head coil. Structural data were acquired using a T1-weighted MPRAGE pulse sequence, using the following parameters: 160 slices/volume, sagittal slice orientation, 12° flip angle, 256×204 matrix. The scan lasted a total of 237 s. Functional data were collected using gradient-echo echo planar imaging with the following parameters: echo time (TE) = 30 ms, repetition time (TR) = 2000 ms, 39 transverse slices with no slice gap acquired in interleaved fashion, voxel dimensions of $3.43\,mm \times 3.43\,mm \times 4.00\,mm$, 70° flip angle, 64×64 matrix. Functional scanning for both tasks lasted 18 min and 12 s in total. Additionally, a T2-fluid attenuated inversion recovery (FLAIR) image was acquired for each participant (except for one MS patient and one control) with the following parameters: TE = 125 ms, TR = 11000 ms, 33 5-mm transverse slices with no gap, $1 \times 1\,mm^3$ in-plane resolution, 120° refocusing angle, 352×212 matrix. The T2-FLAIR image allowed for quantification of lesion burden in MS patients. For a detailed description of T2-FLAIR image processing and results, see the Supplemental Materials, section S.1.

Table 1
Participant demographics, neuropsychometric performance, and MS disease measures.

Characteristic	Healthy controls ($n = 23$)	MS patients ($n = 28$)	*p*-value
Age, mean (SEM)	42.13 (2.56)	47.36 (2.04)	n.s.
Sex, *n* (%)			
Male	6 (26.09%)	5 (17.86%)	–
Female	17 (73.91%)	23 (82.14%)	n.s.
Handedness, *n* (%)			
Right	23 (100%)	28 (100%)	–
SDMT, mean correct (SEM)	58.26 (1.44)	51.88 (2.52)	0.046
PASAT, mean correct (SEM)	49.96 (1.69)	45.84 (2.28)	0.176
Box completion, mean correct (SEM)	55.65 (2.04)	46.60 (2.41)	0.009
Trails A, mean RT (SEM)	21.07 (1.09)	27.51 (2.04)	0.013
Trails B, mean RT (SEM)	40.98 (1.95)	64.99 (9.43)	0.028
EDSS, mean score (SEM)	–	2.78 (0.35)	–
MFIS, mean score (SEM)	–	28.65 (2.49)	–
Lesion burden, mean volume in mm^3 (SEM)	–	15264.60 (2521.91)	

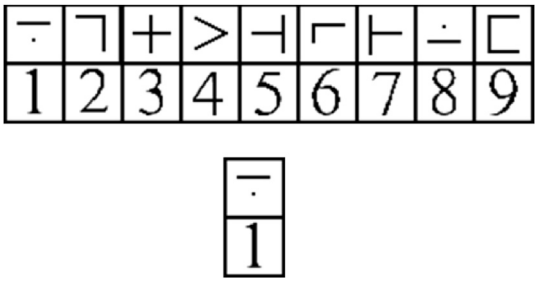

Fig. 2. Sample stimuli from a single trial of the DSST.

Data processing pipeline

Functional data were converted from the Philips PAR/REC proprietary format into the HEAD/BRIK format used by AFNI (Analysis of Functional NeuroImages; Cox, 1996). The functional volumes were then preprocessed to correct for slice timing and realigned to the initial functional volume using a rigid-body transformation to minimize effects of participant motion in the scanner. Motion parameter files for each scanning run were reviewed to ensure motion did not exceed half the length of one voxel on its shortest side (1.71 mm). The MPRAGE structural image was skull-stripped, and functional volumes were aligned to the MPRAGE image. Functional data were then high-pass filtered (0.015625 Hz), eliminating a significant portion of the noise spectrum (<.008 Hz), and spatially smoothed using a Gaussian kernel (FWHM = 6 mm) to increase the signal-to-noise ratio of the data. Extra-cranial noise was removed by masking out voxels that were either located outside of the anatomical brain region or exhibited a high degree of functional signal loss. Participants' structural scans were warped to the Colin TTN27 template, and participants' functional data were then warped to their structural scans within Talairach space using the *@auto_tlrc* program in AFNI. Spatial normalization allowed for demarcations of regions of interest (ROIs) using standard stereotaxic coordinates. All functional and anatomical data were visually inspected before and after preprocessing for artifacts and data processing issues. Preprocessed functional data were then analyzed for each participant using a general linear model (AFNI's 3dDeconvolve command; Ward, 2000).

ROIs were delineated in Talairach space using the AFNI Talairach Daemon. This method yielded a cortical map of three bilateral ROIs: Brodmann's area 4 (BA 4; Brodmann, 1909/2006), composed of precentral gyrus/primary motor cortex, BA 17, composed of striate cortex/primary visual cortex, and BA 9, composed of dorsolateral prefrontal cortex. ROI selection was determined *a priori* and motivated by each region's involvement in the tasks participants completed in the scanner, based on comparable tasks used in previous studies that measured BOLD in primary motor cortex (e.g., Aguirre, Zarahn, & D'Esposito, 1998; D'Esposito et al., 1999; Handwerker, Ollinger, & D'Esposito, 2004), primary visual cortex (e.g., Boynton et al., 1996; Dale and Buckner, 1997; Handwerker, Ollinger, & D'Esposito, 2004), and prefrontal cortex (e.g., DeLuca et al., 2008; Genova et al., 2009; Hubbard et al., 2016b; Leavitt et al., 2011; Rypma et al., 1999, 2006, 2007; Turner et al., 2016).

HRF spline fitting

The spline-fitting method used a finite number of basis functions to permit modeling of participant-specific HRFs, without requiring assumptions that the contour of individual participants' HRFs conform to a canonical shape. The HRF was modeled from baseline during a window of time beginning at stimulus onset using cubic Hermite spline interpolation, fitting piecewise functions for each participant HRF and overall group HRF using BOLD signal calculated at eight time-points, spaced equally at intervals of two seconds (1 TR). These parameter estimates represented percent signal change from baseline, beginning at stimulus onset (t_0) and extending 14 s (t_7) past the initial event (e.g., Dale and Buckner, 1997). This resulted in a maximal fit of the function to the data ($R^2 = 1$ in all cases) and resulted in smooth curves approximating each HRF, within unilateral and bilateral ROIs for each task.

HRF shape differences

Canonicality

A canonical HRF is one that follows the general contour of a standard impulse response function. One caveat to using an approach that minimizes shape assumptions is that non-canonical HRFs are possible, depending on the time course of the BOLD signal. HRFs were categorized as either canonical or non-canonical using the following criteria. A function was deemed canonical unless it met any one of the following criteria to be deemed non-canonical: (1) the spline-fit function contained more than three critical points (i.e., the points at which the slope of the fit function changes direction), (2) the spline-fit function contained only a single critical point, or (3) the maximum of the function occurred beyond the second critical point.

Metrics

We used two metrics to isolate quantifiable differences in overall HRF shape (see Fig. 1). The first metric was peak amplitude, the critical point of the HRF with the maximum value. The second metric was time-to-peak (TTP), the point in time at which each HRF reached peak amplitude. Metrics were calculated using MATLAB code written by one of the authors (MT). Because spline functions can exhibit increased curvature nearer to boundary knots (t_0 and t_7), HRF metrics for each group and individual participant were visually inspected to ensure each metric was appropriately measured.

Results

Performance

RT data for the BPT were analyzed for 45 of the 51 participants, as equipment failure caused loss of data for six participants ($n_{Patient} = 3$; $n_{Control} = 3$). Patients and healthy controls showed similar performance on the BPT as measured by RT ($M_{Patient} = 386.26$ [$SEM = 9.54$] vs. $M_{Control} = 374.37$ [$SEM = 16.67$]), $t(43) = .65$, $p = 0.520$. DSST performance accuracy was not significantly different between MS patients and healthy controls ($M_{Patient} = 93.24\%$ [$SEM = .010$] vs. $M_{Control} = 94.97\%$ [$SEM = .004$]), $t(36.90) = -1.51$, $p = 0.141$. MS patients were significantly slower on the DSST compared to healthy controls ($M_{Patient} = 1804.00$ [$SEM = 61.64$] vs. $M_{Control} = 1595.11$ [$SEM = 57.64$]), $t(49.86) = 2.42$, $p < 0.019$. Results of tests from the neuropsychometric battery are listed in Table 1.

HRF shape and performance

Individual and group HRFs modeled in each ROI during both BPT and DSST performance are illustrated in Fig. 3.

Canonicality

A two-proportion Z-test revealed a significantly greater rate of non-canonical HRFs across all regions (visual, motor, and prefrontal cortex) in MS patients ($P_{Patient} = 32.14\%$, 95% CI [28.21%, 36.34%]) and controls ($P_{Control} = 25.12\%$, [21.18%, 29.51%]), $Z = -2.358$, $p < 0.018$. These results support our hypothesis that MS-related neural-vascular coupling changes are reflected in the shape of the HRF. In subsequent analyses, we quantitatively assessed HRF shape differences to ascertain precisely which metrics differed between groups.

Metrics

To test each of our hypotheses, that (1) HRF canonicality (as measured by peak amplitude and TTP) will differ between MS patients and controls, and (2) HRF metrics will be more associated with processing speed in MS patients than in controls, we utilized multiple regression to predict each HRF Metric from Group and RT separately for BA 4 and BA 17 during BPT performance, and for BA 9 during DSST performance.

Peak amplitude. In MS patients, peak amplitude was reduced compared to healthy controls in BA 17 during BPT performance, and in BA 9 during DSST performance. During BPT performance, there was a significant main effect of Group in BA 17, $F(1,41) = 7.71$, $p < 0.008$. During DSST performance there was a significant main effect of Group in BA 9, $F(1,47) = 10.77$, $p < 0.002$ (see Fig. 4). No other effects were significant

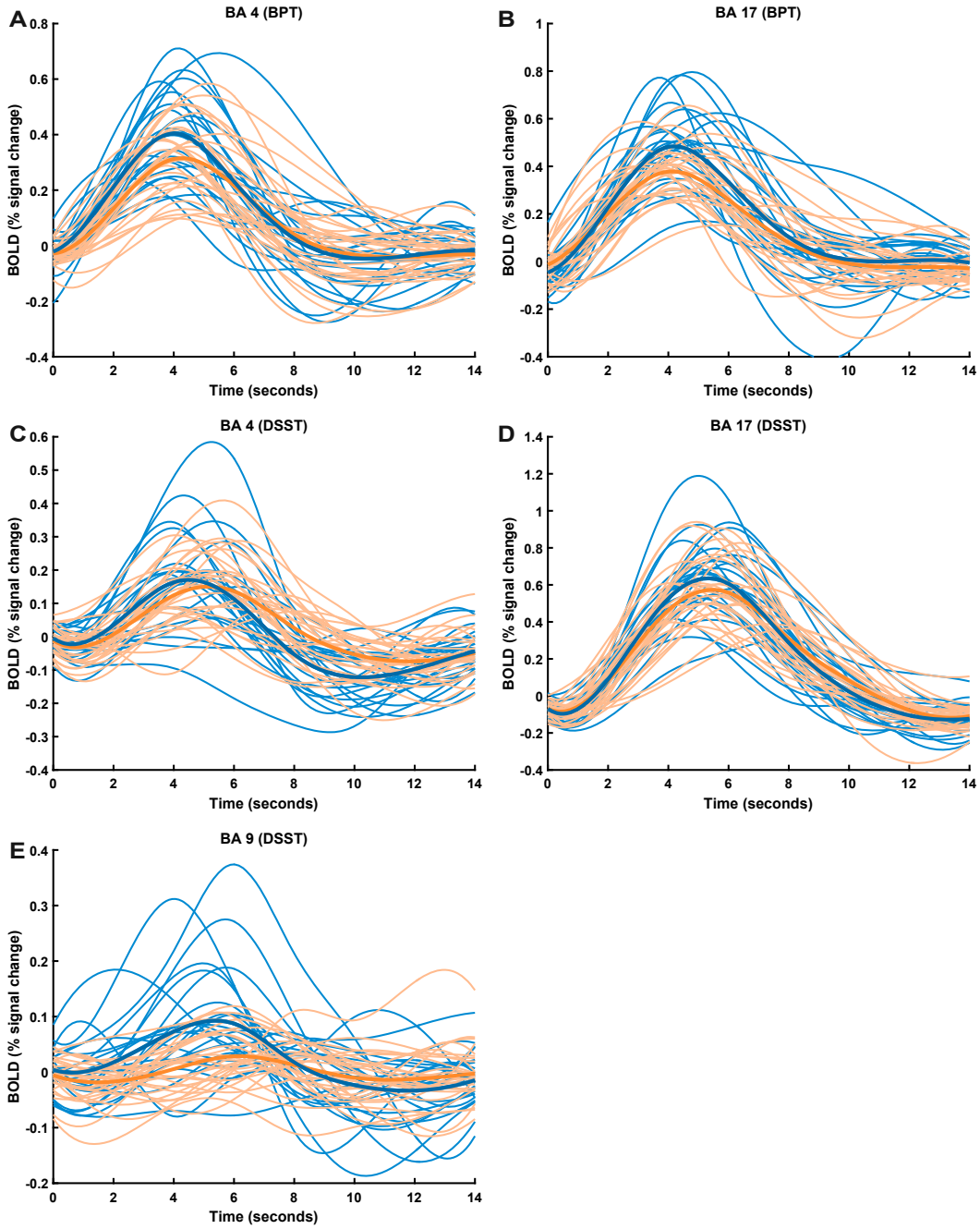

Fig. 3. Individual and group HRFs modeled in bilateral (A) BA 4 during BPT performance, (B) BA 17 during BPT performance, (C) BA 4 during DSST performance, (D) BA 9 during DSST performance, and (E) BA 17 during DSST performance. Individual HRFs are in lighter blue (healthy controls) and orange (MS patients), and group HRFs are darker, bolder curves.

(all $ps > 0.05$).

TTP. In MS patients, TTP was longer compared to healthy controls only in BA 9 during DSST performance. There was a significant main effect of Group, $F(1,47) = 6.27$, $p < 0.016$. TTP was also longer for slower participants than faster participants. There was a significant main effect of RT, $F = 4.77$, $p < 0.034$. This effect was greater in the MS group than in the control group. There was a significant Group × RT interaction, $F = 5.78$, $p < 0.020$ (see Fig. 4).

Medication effects. Multivariate analysis of variance was used to determine whether MS immunomodulatory medications significantly affected any HRF shape metrics. Across all tasks, regions, and metrics, no significant effects of medication were observed (all $ps > 0.05$, uncorrected).

Discussion

In this study, we compared BOLD-HRFs between MS patients and controls without existing parametric canonical models. This approach allowed us to assess differences between characteristics of HRFs while minimizing shape assumptions that could bias the ability to estimate BOLD signal. Results suggested a greater likelihood for the HRFs of MS patients to exhibit a departure from canonicality compared to healthy controls. Additionally, analysis of HRF metrics revealed attenuated peak amplitude and greater TTP in task-related ROIs in MS patients relative to

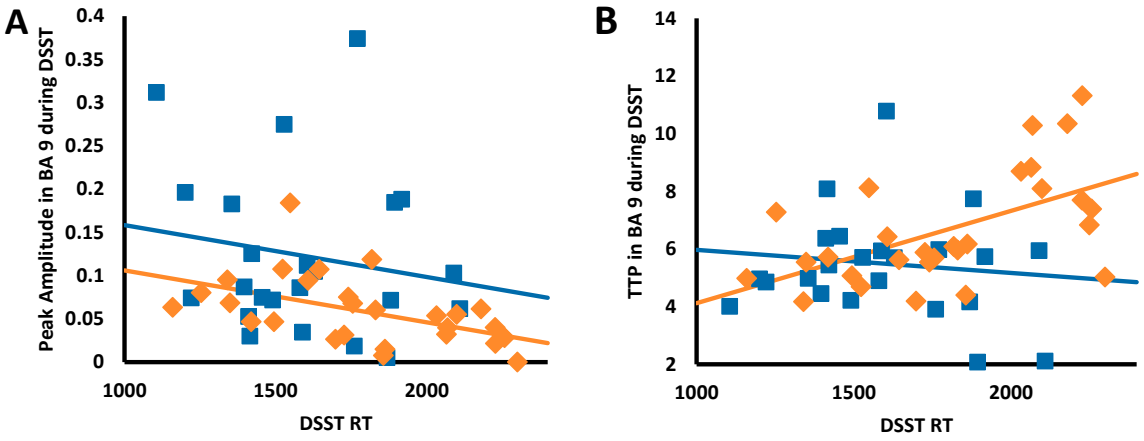

Fig. 4. Relationships between performance (as measured by RT on the DSST) and (A) peak amplitude and (B) TTP in bilateral BA 9. Lines represent the best fit to the data using least-squares linear regression. Healthy controls are in blue, and MS patients are in orange.

controls. Prefrontal TTP was the sole measure predicted by individual differences in processing speed. Specifically, faster TTP was predicted by faster RT, suggesting an important role for vasodilatory speed in processing speed. Based on the fact that BOLD signal measures relative venous deoxyhemoglobin concentration, and that deoxyhemoglobin concentration changes in response to functional hyperemia, the different HRF shape metrics could reflect the critical role that glial cells play in neural-vascular coupling as moderators of nutrient perfusion in response to neurometabolic demand in healthy brains.

The HRF shape characteristics that we compared between MS patients and healthy controls are known to be uniform and reliable in the healthy brain (e.g., Aguirre, Zarahn, & D'Esposito, 1998; Boynton et al., 1996; Buckner et al., 2006; Friston et al., 1998; Lindquist et al., 2009). Such reliability reflects the integrity of glial (e.g., astrocytes; see Haydon and Carmignoto, 2006; Petzold and Murthy, 2011; Rossi, 2006; Takano et al., 2006; and passive diffusion mechanisms; see Cauli and Hamel, 2010) and vascular structures (e.g., endothelium, smooth muscle cells; e.g., Chen et al., 2014; Davis et al., 1998; Hoge et al., 1999; Hutchison et al., 2013a, b; Stefanovic et al., 2004) that facilitate changes in neurometabolic demand. Reductions in this integrity, as we observed in MS, underscore the importance of mechanisms that (1) allow neurons to feed forward their metabolic needs to vasculature via communicating structures (e.g., Attwell et al., 2010; Hillman, 2014), and (2) allow vasculature to feed back oxygen and nutrients to neurons via glial cells (e.g., Lee et al., 2012; Rinholm and Bergersen, 2012), ultimately facilitating neural performance (and, the current results suggest, cognitive performance).

In this study, we tested the hypothesis that dysfunction in underlying physiology in MS could be indexed by departures of HRF shape from canonicality. HRF canonicality was preserved at a greater rate in healthy controls than in MS patients (a group for which glial disruption is known; see Brosnan and Raine, 2013; De Keyser et al., 2008; D'Haeseleer et al., 2011; Gareau et al., 1999; Jukkola et al., 2013; Lassmann, 2003, 2014; Lundgaard et al., 2014; Mulligan and MacVicar, 2004; Trapp and Stys, 2009). Interestingly, HRF variability in all regions tested was greater in healthy controls relative to MS patients (see Fig. 3). This finding might reflect a floor effect in MS patients, where smaller task-related excursions from baseline might result in a narrower envelope through which HRFs may vary across time.

Peak amplitude was lower in MS patients compared to healthy controls, possibly reflecting reduced vascular dilation (e.g., Devor et al., 2005; Metea and Newman, 2006), or a reduced proportion of oxygen extracted from capillary blood (e.g., Griffeth and Buxton, 2011; Hyder et al., 2001; Lu and Van Zijl, 2005; Trapp and Stys, 2009). TTP was higher in MS patients compared to healthy controls, possibly reflecting a delay of the system to reach maximal oxygen perfusion. This delay could be due to either disrupted glial vasodilatory signaling (e.g., Bonakdarpour et al., 2007; Devor et al., 2005; Metea and Newman, 2006), or to differences in the efficiency of oxygen extraction from capillaries (e.g., Griffeth and Buxton, 2011; Hyder et al., 2001; Lu and Van Zijl, 2005; Trapp and Stys, 2009). Immunomodulatory medications did not exert significant effects on any of these metrics. These results suggest that canonical HRFs reflect intact neural-glial-vascular communication, oxygen extraction, and vascular compliance, fundamental to optimal functional hyperemia, neural efficiency, and cognitive performance.

It is worth noting that significant complexity accompanies interpretation of BOLD-HRFs in the context of underlying neural-vascular activity (e.g., Lindquist and Wager, 2007; Lindquist et al., 2009). Measurement of the HRF occurs on a time scale three orders of magnitude greater than that of underlying neuronal activity (Logothetis, 2002). Heterogeneity in the evolution of the HRF through time exists across cortical regions (Aguirre, Zarahn, & D'Esposito, 1998; Handwerker, Ollinger, & D'Esposito, 2004), wherein the relationship between BOLD signal and underlying neural activity is sometimes linear (e.g., Boynton et al., 1996), but sometimes nonlinear (e.g., Birn et al., 2001; Martindale et al., 2005). More advanced techniques, such as calibrated fMRI (that measures both BOLD and cerebral blood flow and permits calculation of cerebral oxygen metabolism; e.g., Hutchison et al., 2013a,b) or combined EEG-fMRI, will be needed to assess the validity of these hypotheses.

The hypothesis that intact communication between neurons, glia, and vasculature is essential to optimal neural performance is supported by relationships we observed between HRF shape metrics and behavioral performance. MS-related physiologic dysfunction reflected in non-canonical HRFs impairs neural performance and, the present results suggest, efficient cognitive performance. While group differences were found in both HRF metrics, processing speed performance exclusively predicted TTP in prefrontal cortex. Further, the effect of processing speed performance was stronger in MS patients than in healthy controls as evidenced by a significant Group × RT interaction effect. This result suggests the hypothesis that mechanisms underlying HRF latency (e.g., delay in functional hyperemia) play a larger role in speed of processing (an ability known to be central to general cognitive performance; Salthouse, 1996; Vernon, 1983) than those underlying peak amplitude (e.g., oxygen extraction).

Earlier work from our lab (Rypma et al., 1999, 2006, 2007; Turner et al., 2016), and from others (e.g., Bachman et al., 2010; Boone et al., 1998; DeLuca et al., 2008; Genova et al., 2009), has localized processing-speed ability to prefrontal cortex, a region not known for frank MS lesions. This result is consistent with others showing that MS pathology exerts pervasive deleterious effects well beyond white-matter lesion sites. Previous research has demonstrated that global attenuation in fractional anisotropy predicted HRF peak amplitude in visual and motor cortex, whereas lesion location in MS patients did not (Hubbard

et al., 2016a). This result, combined with our finding that lesion burden was not related to behavioral performance (see Supplemental Material), suggests that MS-related damage is not limited to lesioned regions, and instead represents dysfunction occurring at a system-wide level. Further work using more advanced white-matter imaging techniques (such as diffusion kurtosis imaging; see e.g., Lu et al., 2006) will be needed to better characterize white-matter-HRF relationships.

There are several caveats to interpretation of our results. First, much remains to be elucidated about MS pathophysiology, which limits the confidence with which we can provide a straightforward interpretation of altered HRF shape. However, strong relationships between HRF shape measures and performance provide compelling evidence that altered hemodynamic processes in instances of white-matter compromise have consequences for cognition. Second, the standard-space analyses that we employed to facilitate like-to-like spatial between-groups comparisons may not account for cortical gray-matter atrophy often seen in neurodegenerative diseases such as MS (Azevedo and Pelletier, 2016; Calabrese et al., 2007, 2009; Fisher et al., 2008; Fisniku et al., 2008; Geurts and Barkhof, 2008; Geurts et al., 2012; Pirko et al., 2007; Vercellino et al., 2009). Calibrated imaging work shows that altered gray-matter metabolism in MS is related to white-matter compromise (Hubbard et al., 2017; see also Varga et al., 2009). More work is certainly needed to disentangle relative influences of white- and gray-matter on HRF shape and cognitive performance. Third, the MS patients scanned in our study were permitted to take their regular courses of medications (e.g., glatiramer acetate, interferon-beta, natalizumab) on the day of their scans. Although we did not observe significant effects of these medications on the HRF, effects of these medications on the BOLD signal remain unknown. Additional work is certainly needed to pursue answers to these unresolved questions.

Imaging studies of MS commonly focus on the involvement of white-matter. Other populations feature differences in white-matter structure relative to healthy young-adult brains. White-matter volume is known to decline, for instance, even as a consequence of healthy aging (e.g., Bartzokis et al., 2003; Bennett et al., 2010; Gunning-Dixon et al., 2009; Salat et al., 1999). Degradation of white-matter integrity is also observed in cases of neurodegeneration other than MS, including Alzheimer's disease (Acosta-Cabronero et al., 2010; Bozzali et al., 2002), Parkinson's disease (Hattori et al., 2012; Rae et al., 2012), and amyotrophic lateral sclerosis (Abrahams et al., 2005; Zhang et al., 2007). Further, a prominent hallmark of healthy brain development in children is maturation of white-matter (e.g., Barnea-Goraly et al., 2005; Klingberg et al., 1999; Mabbott et al., 2006; Nagy et al., 2004). These groups also exhibit cognitive performance differences relative to healthy young adult controls. Such cognitive performance differences provide further evidence for the importance of intact neural-vascular coupling to intact neural performance, and in turn, cognitive performance.

Conclusions

We isolated differences in HRF metrics between MS patients and healthy controls to assess how HRF shape differed between groups, and to assess the extent to which departures from a canonical HRF shape were related to performance differences. The use of an approach that (1) compared healthy individuals to a group with known white-matter damage, and (2) minimized assumptions regarding HRF shape, made this assessment sensitive enough to isolate group differences that might not have been apparent if a standard impulse response function had been used. HRF shape was significantly altered between groups, and was related to processing speed differences. Together, these results provide support for the hypothesis that alterations to glial cell intermediaries are associated with neural-vascular coupling deficits, that are in turn related to reductions in neural function and processing speed. Neural-glial-vascular communication might form the basis for optimal neural performance, and provide a plausible physiological mechanism for processing speed differences between healthy younger, older, and diseased groups.

Conflicts of interest

MT, NAH, DKS, LMH, JLH, JH, JS, and BR are not aware of any potential financial conflicts of interest related to the current study. EF, TF, and DO have received honoraria from speaking engagements with pharmaceutical companies related to Multiple Sclerosis, but unrelated to the current study.

Acknowledgements and funding

This work was supported by the Dianne Cash Predoctoral Fellowship (to MT), the Friends of Brain Health and the Linda and Joel Roebuck Distinguished New Scientist endowments (to NAH), the National Multiple Sclerosis Society (RG4453A1/2 to BR and EF), and the National Institutes of Health (1R01AG047972 and 1R01AG029523 to BR). The content does not necessarily reflect the position or the policy of the Federal government or the sponsoring agencies, and no official endorsement should be inferred.

Appendix A. Supplementary data

Supplementary data related to this article can be found at https://doi.org/10.1016/j.neuroimage.2017.12.081.

References

Abrahams, S., Leigh, P.N., Goldstein, L.H., 2005. Cognitive change in ALS A prospective study. Neurology 64 (7), 1222–1226.
Ackerman, P.L., Beier, M.E., Boyle, M.D., 2002. Individual differences in working memory within a nomological network of cognitive and perceptual speed abilities. J. Exp. Psychol. Gen. 131 (4), 567.
Acosta-Cabronero, J., Williams, G.B., Pengas, G., Nestor, P.J., 2010. Absolute diffusivities define the landscape of white matter degeneration in Alzheimer's disease. Brain 133 (2), 529–539.
Aguirre, G.K., Zarahn, E., D'Esposito, M., 1998. The variability of human, BOLD hemodynamic responses. Neuroimage 8 (4), 360–369.
Aizenstein, H.J., Clark, K.A., Butters, M.A., Cochran, J., Stenger, V.A., Meltzer, C.C., Reynolds, C.F., Carter, C.S., 2004. The BOLD hemodynamic response in healthy aging. J. Cognit. Neurosci. 16 (5), 786–793.
Ances, B.M., Liang, C.L., Leontiev, O., Perthen, J.E., Fleisher, A.S., Lansing, A.E., Buxton, R.B., 2009. Effects of aging on cerebral blood flow, oxygen metabolism, and blood oxygenation level dependent responses to visual stimulation. Hum. Brain Mapp. 30 (4), 1120–1132.
Attwell, D., Buchan, A.M., Charpak, S., Lauritzen, M., Macvicar, B.A., Newman, E.A., 2010. Glial and neuronal control of brain blood flow. Nature 468 (7321), 232–243, 2010 Nov 11.
Azevedo, C.J., Pelletier, D., 2016. Whole-brain atrophy: ready for implementation into clinical decision-making in multiple sclerosis? Curr. Opin. Neurol. 29 (3), 237–242.
Bachman, P., Reichenberg, A., Rice, P., Woolsey, M., Chaves, O., Martinez, D., Maples, N., Velligan, D.I., Glahn, D.C., 2010. Deconstructing processing speed deficits in schizophrenia: application of a parametric digit symbol coding test. Schizophr. Res. 118 (1), 6–11.
Barnea-Goraly, N., Menon, V., Eckert, M., Tamm, L., Bammer, R., Karchemskiy, A., Dant, C.C., Reiss, A.L., 2005. White matter development during childhood and adolescence: a cross-sectional diffusion tensor imaging study. Cerebr. Cortex 15 (12), 1848–1854.
Bartzokis, G., Cummings, J.L., Sultzer, D., Henderson, V.W., Nuechterlein, K.H., Mintz, J., 2003. White matter structural integrity in healthy aging adults and patients with Alzheimer disease: a magnetic resonance imaging study. Arch. Neurol. 60 (3), 393–398.
Bennett, I.J., Madden, D.J., Vaidya, C.J., Howard, D.V., Howard Jr., J.H., 2010. Age-related differences in multiple measures of white matter integrity: a diffusion tensor imaging. Hum. Brain Mapp. 31 (3), 378–390, 2010 Mar.
Birn, R.M., Saad, Z.S., Bandettini, P.A., 2001. Spatial heterogeneity of the nonlinear dynamics in the FMRI BOLD response. Neuroimage 14 (4), 817–826.
Blanco, V.M., Stern, J.E., Filosa, J.A., 2008. Tone-dependent vascular responses to astrocyte-derived signals. Am. J. Physiol. Heart Circ. Physiol. 294 (6), H2855–H2863.
Bonakdarpour, B., Parrish, T.B., Thompson, C.K., 2007. Hemodynamic response function in patients with stroke-induced aphasia: implications for fMRI data analysis. Neuroimage 36 (2), 322–331.
Bonnet, M.C., Allard, M., Dilharreguy, B., Deloire, M., Petry, K.G., Brochet, B., 2010. Cognitive compensation failure in multiple sclerosis. Neurology 75 (14), 1241–1248.
Bonzano, L., Pardini, M., Mancardi, G.L., Pizzorno, M., Roccatagliata, L., 2009. Structural connectivity influences brain activation during PVSAT in multiple sclerosis. Neuroimage 44 (1), 9–15.

Boone, K.B., Pontón, M.O., Gorsuch, R.L., González, J.J., Miller, B.L., 1998. Factor analysis of four measures of prefrontal lobe functioning. Arch. Clin. Neuropsychol. 13 (7), 585–595.
Bowen, J., Gibbons, L., Gianas, A., Kraft, G.H., 2001. Self-administered Expanded Disability Status Scale with functional system scores correlates well with a physician-administered test. Mult. Scler. J. 7 (3), 201–206.
Boynton, G., Engel, S., Glover, G., Heeger, D., 1996. Linear systems analysis of functional magnetic resonance imaging in human V1. J. Neurosci. 4207–4221.
Bozzali, M., Falini, A., Franceschi, M., Cercignani, M., Zuffi, M., Scotti, G., Comi, G., Filippi, M., 2002. White matter damage in Alzheimer's disease assessed in vivo using diffusion tensor magnetic resonance imaging. J. Neurol. Neurosurg. Psychiatr. 72 (6), 742–746.
Brodmann, K., 1909/2006. Brodmann's Localisation in the Cerebral Cortex, vol. 2005. Springer, US. https://doi.org/10.1007/b138298.
Brooks, D.J., Leenders, K.L., Head, G., Marshall, J., Legg, N.J., Jones, T., 1984. Studies on regional cerebral oxygen utilisation and cognitive function in multiple sclerosis. J. Neurol. Neurosurg. Psychiatr. 47 (11), 1182–1191.
Brosnan, C.F., Raine, C.S., 2013. The astrocyte in multiple sclerosis revisited. Glia 61 (4), 453–465.
Brown, G.C., 2007. Nitric oxide and mitochondria. Front. Biosci. 12 (6), 1024–1033.
Brown, G.C., 2010. Nitric oxide and neuronal death. Nitric Oxide 23 (3), 153–165.
Brown, G.C., Bal-Price, A., 2003. Inflammatory neurodegeneration mediated by nitric oxide, glutamate, and mitochondria. Mol. Neurobiol. 27 (3), 325–355.
Brown, G.C., Borutaite, V., 2002. Nitric oxide inhibition of mitochondrial respiration and its role in cell death. Free Radic. Biol. Med. 33 (11), 1440–1450.
Buckner, R.L., Snyder, A.Z., Sanders, A.L., Raichle, M.E., Morris, J.C., 2006. Functional Brain Imaging of Young, Nondemented, and Demented Older Adults. MIT Press.
Buxton, R.B., Uludağ, K., Dubowitz, D.J., Liu, T.T., 2004. Modeling the hemodynamic response to brain activation. Neuroimage 23, S220–S233.
Calabrese, M., Atzori, M., Bernardi, V., Morra, A., Romualdi, C., Rinaldi, L., McAuliffe, M.J.M., Barachino, L., Perini, P., Fischl, B., Battistin, L., Gallo, P., 2007. Cortical atrophy is relevant in multiple sclerosis at clinical onset. J. Neurol. 254 (9), 1212–1220.
Calabrese, M., Agosta, F., Rinaldi, F., Mattisi, I., Grossi, P., Favaretto, A., Atzori, M., Bernardi, V., Barachino, L., Rinaldi, L., Perini, P., Gallo, P., Filippi, M., 2009. Cortical lesions and atrophy associated with cognitive impairment in relapsing-remitting multiple sclerosis. Arch. Neurol. 66 (9), 1144–1150.
Calhoun, V.D., Kiehl, K.A., Liddle, P.F., Pearlson, G.D., 2004. Aberrant localization of synchronous hemodynamic activity in auditory cortex reliably characterizes schizophrenia. Biol. Psychiatr. 55 (8), 842–849.
Carew, J.D., Wahba, G., Xie, X., Nordheim, E.V., Meyerand, M.E., 2003. Optimal spline smoothing of fMRI time series by generalized cross-validation. Neuroimage 18 (4), 950–961.
Carmignoto, G., Gómez-Gonzalo, M., 2010. The contribution of astrocyte signalling to neurovascular coupling. Brain Res. Rev. 63 (1), 138–148.
Cauli, B., Hamel, E., 2010. Revisiting the role of neurons in neurovascular coupling. Front. Neuroenergetics 2 (9), 1–8.
Chen, B.R., Kozberg, M.G., Bouchard, M.B., Shaik, M.A., Hillman, E.M., 2014. A critical role for the vascular endothelium in functional neurovascular coupling in the brain. J. Am. Heart Assoc. 3 (3), e000787.
Chung, S.C., Iwaki, S., Tack, G.R., Yi, J.H., You, J.H., Kwon, J.H., 2006. Effect of 30% oxygen administration on verbal cognitive performance, blood oxygen saturation and heart rate. Appl. Psychophysiol. Biofeedback 31 (4), 281–293.
Cox, R.W., 1996. AFNI: software for analysis and visualization of functional magnetic resonance neuroimages. Comput. Biomed. Res. 29 (3), 162–173, 1996 Jun.
Dale, A.M., Buckner, R.L., 1997. Selective averaging of rapidly presented individual trials using fMRI. Hum. Brain Mapp. 5 (5), 329–340.
Davis, T.L., Kwong, K.K., Weisskoff, R.M., Rosen, B.R., 1998. Calibrated functional MRI: mapping the dynamics of oxidative metabolism. Proc. Natl. Acad. Sci. U. S. A. 95 (4), 1834–1839, 1998 Feb 17.
De Keyser, J., Steen, C., Mostert, J.P., Koch, M.W., 2008. Hypoperfusion of the cerebral white matter in multiple sclerosis: possible mechanisms and pathophysiological significance. J. Cerebr. Blood Flow Metabol. 28, 1645–1651.
De Keyser, J., Wilczak, N., Leta, R., Streetland, C., 1999. Astrocytes in multiple sclerosis lack beta-2 adrenergic receptors. Neurology 53 (8), 1628.
Debernard, L., Melzer, T.R., Van Stockum, S., Graham, C., Wheeler-Kingshott, C.A., Dalrymple-Alford, J.C., Miller, D.H., Mason, D.F., 2013. Reduced grey matter perfusion without volume loss in early relapsing-remitting multiple sclerosis. J. Neurol. Neurosurg. Psychiatr. 85 (5), 544–551 jnnp-2013.
DeLuca, J., Genova, H.M., Hillary, F.G., Wylie, G., 2008. Neural correlates of cognitive fatigue in multiple sclerosis using functional MRI. J. Neurol. Sci. 270 (1), 28–39.
Devor, A., Ulbert, I., Dunn, A.K., Narayanan, S.N., Jones, S.R., Andermann, M.L., Boas, D.A., Dale, A.M., 2005. Coupling of the cortical hemodynamic response to cortical and thalamic neuronal activity. Proc. Natl. Acad. Sci. U. S. A. 102 (10), 3822–3827.
Dineen, R.A., Vilisaar, J., Hlinka, J., Bradshaw, C.M., Morgan, P.S., Constantinescu, C.S., Auer, D.P., 2009. Disconnection as a mechanism for cognitive dysfunction in multiple sclerosis. Brain 132 (1), 239–249.
D'Esposito, M., Zarahn, E., Aguirre, G.K., Rypma, B., 1999. The effect of normal aging on the coupling of neural activity to the bold hemodynamic response. Neuroimage 10 (1), 6–14.
D'Esposito, M., Deouell, L.Y., Gazzaley, A., 2003. Alterations in the BOLD fMRI signal with ageing and disease: a challenge for neuroimaging. Nat. Rev. Neurosci. 4 (11), 863–872.
D'Haeseleer, M., Cambron, M., Vanopdenbosch, L., De Keyser, J., 2011. Vascular aspects of multiple sclerosis. Lancet Neurol. 10 (7), 657–666, 2011 Jul.
Fisher, E., Lee, J.C., Nakamura, K., Rudick, R.A., 2008. Gray matter atrophy in multiple sclerosis: a longitudinal study. Ann. Neurol. 64 (3), 255–265.
Fisk, J.D., Ritvo, P.G., Ross, L., Haase, D.A., Marrie, T.J., Schlech, W.F., 1994. Measuring the functional impact of fatigue: initial validation of the fatigue impact scale. Clin. Infect. Dis. 18 (Supplement_1), S79–S83.
Fisniku, L.K., Chard, D.T., Jackson, J.S., Anderson, V.M., Altmann, D.R., Miszkiel, K.A., Thompson, A.J., Miller, D.H., 2008. Gray matter atrophy is related to long-term disability in multiple sclerosis. Ann. Neurol. 64 (3), 247–254.
Friston, K.J., Fletcher, P., Josephs, O., Holmes, A.W., Rugg, M.D., Turner, R., 1998. Event-related fMRI: characterizing differential responses. Neuroimage 7 (1), 30–40.
Gareau, P.J., Gati, J.S., Menon, R.S., Lee, D., Rice, G., Mitchell, J.R., Mandelfino, P., Karlik, S.J., 1999. Reduced visual evoked responses in multiple sclerosis patients with optic neuritis: comparison of functional magnetic resonance imaging and visual evoked potentials. Mult. Scler. J. 5 (3), 161–164.
Ge, Y., Law, M., Johnson, G., Herbert, J., Babb, J.S., Mannon, L.J., Grossman, R.I., 2005. Dynamic susceptibility contrast perfusion MR imaging of multiple sclerosis lesions: characterizing hemodynamic impairment and inflammatory activity. Am. J. Neuroradiol. 26 (6), 1539–1547.
Genova, H., Hillary, F., Wylie, G., Rypma, B., Deluca, J., 2009. Examination of processing speed deficits in multiple sclerosis using functional magnetic resonance imaging. J. Int. Neuropsychol. Soc. 383–393.
Geurts, J.J., Barkhof, F., 2008. Grey matter pathology in multiple sclerosis. Lancet Neurol. 7 (9), 841–851.
Geurts, J.J., Calabrese, M., Fisher, E., Rudick, R.A., 2012. Measurement and clinical effect of grey matter pathology in multiple sclerosis. Lancet Neurol. 11 (12), 1082–1092.
Gibbons, R.D., Lazar, N.A., Bhaumik, D.K., Sclove, S.L., Chen, H.Y., Thulborn, K.R., Sweeney, J.A., Hur, K., Patterson, D., 2004. Estimation and classification of fMRI hemodynamic response patterns. Neuroimage 808–814.
Glover, G.H., 1999. Deconvolution of impulse response in event-related bold fmri 1. Neuroimage 9 (4), 416–429.
Goutte, C., Nielsen, F.A., Hansen, K.H., 2000. Modeling the hemodynamic response in fMRI using smooth FIR filters. IEEE Trans. Med. Imag. 19 (12), 1188–1201.
Griffeth, V.E., Buxton, R.B., 2011. A theoretical framework for estimating cerebral oxygen metabolism changes using the calibrated-BOLD method: modeling the effects of blood volume distribution, hematocrit, oxygen extraction fraction, and tissue signal properties on the BOLD signal. Neuroimage 58 (1), 198–212.
Gronwall, D.M.A., 1977. Paced auditory serial-addition task: a measure of recovery from concussion. Percept. Mot. Skills 44 (2), 367–373.
Gunning-Dixon, F.M., Brickman, A.M., Cheng, J.C., Alexopoulos, G.S., 2009. Aging of cerebral white matter: a review of MRI findings. Int. J. Geriatr. Psychiatr. 24 (2), 109–117.
Handwerker, D.A., Ollinger, J.M., D'Esposito, M., 2004. Variation of BOLD hemodynamic responses across subjects and brain regions and their effects on statistical analyses. Neuroimage 21 (4), 1639–1651.
Haselhorst, R., Kappos, L., Bilecen, D., Scheffler, K., Möri, D., Radü, E.W., Seelig, J., 2000. Dynamic susceptibility contrast MR imaging of plaque development in multiple sclerosis: application of an extended blood-brain barrier leakage correction. J. Magn. Reson. Imag. 11 (5), 495–505.
Hattori, T., Orimo, S., Aoki, S., Ito, K., Abe, O., Amano, A., Sato, R., Sakai, K., Mizusawa, H., 2012. Cognitive status correlates with white matter alteration in Parkinson's disease. Hum. Brain Mapp. 33 (3), 727–739.
Haydon, P.G., Carmignoto, G., 2006. Astrocyte control of synaptic transmission and neurovascular coupling. Physiol. Rev. 86 (3), 1009–1031.
Henson, R.N., Price, C.J., Rugg, M.D., Turner, R., Friston, K.J., 2002. Detecting latency differences in event-related BOLD responses: application to words versus nonwords and initial versus repeated face presentations. Neuroimage 15 (1), 83–97.
Hillman, E.M., 2014. Coupling mechanism and significance of the BOLD signal: a status report. Annu. Rev. Neurosci. 37, 161–181.
Hoge, R.D., Atkinson, J., Gill, B., Crelier, G.R., Marrett, S., Pike, G.B., 1999. Investigation of BOLD signal dependence on cerebral blood flow and oxygen consumption: the deoxyhemoglobin dilution model. Magn. Reson. Med. 42 (5), 849–863, 1999 Nov.
Hubbard, N.A., Turner, M., Hutchison, J.L., Ouyang, A., Strain, J., Oasay, L., Sundaram, S., Davis, S., Remington, G., Brigante, R., Huang, H., Hart Jr., J., Frohman, T., Frohman, E., Biswal, B.B., Rypma, B., 2016a. Multiple sclerosis-related white matter microstructural change alters the BOLD hemodynamic response. J. Cerebr. Blood Flow Metabol. 36 (11), 1872–1884.
Hubbard, N.A., Hutchison, J.L., Turner, M.P., Sundaram, S., Oasay, L., Robinson, D., Strain, J., Weaver, T., Davis, S.L., Remington, G.M., Huang, H., Biswal, B.B., Hart Jr., J., Frohman, T.C., Frohman, E.M., Rypma, B., 2016b. Asynchrony in executive networks predicts cognitive slowing in multiple sclerosis. Neuropsychology 30 (1), 75.
Hubbard, N.A., Turner, M.P., Ouyang, M., Himes, L., Thomas, B.P., Hutchison, J.L., Faghihahmadabadi, S., Davis, S.L., Strain, J.F., Spence, J., Krawczyk, D.C., Huang, H., Lu, H., Hart Jr., J., Frohman, T.C., Frohman, E.M., Okuda, D.T., Rypma, B., 2017. Calibrated imaging reveals altered grey matter metabolism related to white matter microstructure and symptom severity in multiple sclerosis. Hum. Brain Mapp. 38 (11), 5375–5390.
Huettel, S.A., Singerman, J.D., McCarthy, G., 2001. The effects of aging upon the hemodynamic response measured by functional MRI. Neuroimage 13 (1), 161–175.
Hutchison, J.L., Lu, H., Rypma, B., 2013a. Neural mechanisms of age-related slowing: the ΔCBF/ΔCMRO2 ratio mediates age-differences in BOLD signal and human performance. Cerebr. Cortex 23 (10), 2337–2346 bhs233.
Hutchison, J.L., Shokri-Kojori, E., Lu, H., Rypma, B., 2013b. A BOLD perspective on age-related neurometabolic-flow coupling and neural efficiency changes in human visual cortex. Front. Psychol. 4.

Hyder, F., Kida, I., Behar, K.L., Kennan, R.P., Maciejewski, P.K., Rothman, D.L., 2001. Quantitative functional imaging of the brain: towards mapping neuronal activity by BOLD fMRI. NMR Biomed. 14 (7–8), 413–431.
Iadecola, C., 2017. The neurovascular unit coming of age: a journey through neurovascular coupling in health and disease. Neuron 96 (1), 17–42.
Jukkola, P., Guerrero, T., Gray, V., Gu, C., 2013. Astrocytes differentially respond to inflammatory autoimmune insults and imbalances of neural activity. Acta Neuropathol. Commun. 1 (1), 70.
Kern, K.C., Ekstrom, A.D., Suthana, N.A., Giesser, B.S., Montag, M., Arshanapalli, A., Bookheimer, S.Y., Sicotte, N.L., 2012. Fornix damage limits verbal memory functional compensation in multiple sclerosis. Neuroimage 59 (3), 2932–2940.
Klingberg, T., Vaidya, C.J., Gabrieli, J.D., Moseley, M.E., Hedehus, M., 1999. Myelination and organization of the frontal white matter in children: a diffusion tensor MRI study. Neuroreport 10 (13), 2817–2821.
Kwong, K.K., Belliveau, J.W., Chesler, D.A., Goldberg, I.E., Weisskoff, R.M., Poncelet, B.P., Kennedy, D.N., Hoppel, B.E., Cohen, M.S., Turner, R., 1992. Dynamic magnetic resonance imaging of human brain activity during primary sensory stimulation. Proc. Natl. Acad. Sci. U. S. A. 89 (12), 5675–5679.
Lassmann, H., 2003. Hypoxia-like tissue injury as a component of multiple sclerosis lesions. J. Neurol. Sci. 206 (2), 187–191.
Lassmann, H., 2014. Mechanisms of white matter damage in multiple sclerosis. Glia 62 (11), 1816–1830.
Law, M., Saindane, A.M., Ge, Y., Babb, J.S., Johnson, G., Mannon, L.J., Herbert, J., Grossman, R.I., 2004. Microvascular abnormality in relapsing-remitting multiple sclerosis: perfusion MR imaging findings in normal-appearing white matter. Radiology 231 (3), 645–652.
Leavitt, V.M., Lengenfelder, J., Moore, N.B., Chiaravalloti, N.D., DeLuca, J., 2011. The relative contributions of processing speed and cognitive load to working memory accuracy in multiple sclerosis. J. Clin. Exp. Neuropsychol. 33 (5), 580–586.
Lee, M., Reddy, H., Johansen-Berg, H., Pendlebury, S., Jenkinson, M., Smith, S., Palace, J., Matthews, P.M., 2000. The motor cortex shows adaptive functional changes to brain injury from multiple sclerosis. Ann. Neurol. 47 (5), 606–613.
Lee, Y., Morrison, B.M., Li, Y., Lengacher, S., Farah, M.H., Hoffman, P.N., Liu, Y., Tsingalia, A., Jin, L., Zhang, P.W., Pellerin, L., Magistretti, P.J., Rothstein, J.D., 2012. Oligodendroglia metabolically support axons and contribute to neurodegeneration. Nature 487 (7408), 443.
Lindquist, M.A., Wager, T.D., 2007. Validity and power in hemodynamic response modeling: a comparison study and a new approach. Hum. Brain Mapp. 28 (8), 764–784.
Lindquist, M.A., Loh, J.M., Atlas, L.Y., Wager, T.D., 2009. Modeling the hemodynamic response function in fMRI: efficiency, bias and mis-modeling. Neuroimage 45 (1), S187–S198.
Logothetis, N., 2002. The neural basis of the blood-oxygen-level-dependent functional magnetic resonance imaging signal. Philos. Trans. R. Soc. London, Ser. B 1003–1037.
Lu, H., Van Zijl, P., 2005. Experimental measurement of extravascular parenchymal BOLD effects and tissue oxygen extraction fractions using multi-echo VASO fMRI at 1.5 and 3.0 T. Magn. Reson. Med. 53 (4), 808–816.
Lu, H., Jensen, J.H., Ramani, A., Helpern, J.A., 2006. Three-dimensional characterization of non-gaussian water diffusion in humans using diffusion kurtosis imaging. NMR Biomed. 19 (2), 236–247.
Lundgaard, I., Osório, M.J., Kress, B.T., Sanggaard, S., Nedergaard, M., 2014. White matter astrocytes in health and disease. Neuroscience 276, 161–173.
Lycke, J., Wikkelsö, C., Bergh, A.C., Jacobsson, L., Andersen, O., 1993. Regional cerebral blood flow in multiple sclerosis measured by single photon emission tomography with technetium-99m hexamethyl-propyleneamine oxime. Eur. Neurol. 33 (2), 163–167.
Mabbott, D.J., Noseworthy, M., Bouffet, E., Laughlin, S., Rockel, C., 2006. White matter growth as a mechanism of cognitive development in children. Neuroimage 33 (3), 936–946.
Martin, C., Martindale, J., Berwick, J., Mayhew, J., 2006. Investigating neural–hemodynamic coupling and the hemodynamic response function in the awake rat. Neuroimage 32 (1), 33–48.
Martindale, J., Berwick, J., Martin, C., Kong, Y., Zheng, Y., Mayhew, J., 2005. Long duration stimuli and nonlinearities in the neural–haemodynamic coupling. J. Cerebr. Blood Flow Metabol. 25 (5), 651–661.
Marshall, O., Lu, H., Brisset, J.C., Xu, F., Liu, P., Herbert, J., Grossman, R.I., Ge, Y., 2014. Impaired cerebrovascular reactivity in multiple sclerosis. JAMA Neurol. 71 (10), 1275–1281.
Maus, B., van Breukelen, G.J., Goebel, R., Berger, M.P., 2012. Optimal design for nonlinear estimation of the hemodynamic response function. Hum. Brain Mapp. 33 (6), 1253–1267.
Metea, M.R., Newman, E.A., 2006. Glial cells dilate and constrict blood vessels: a mechanism of neurovascular coupling. J. Neurosci. 26 (11), 2862–2870.
Mohtasib, R.S., Lumley, G., Goodwin, J.A., Emsley, H.C., Sluming, V., Parkes, L.M., 2012. Calibrated fMRI during a cognitive Stroop task reveals reduced metabolic response with increasing age. Neuroimage 59 (2), 1143–1151.
Mulholland, A.D., Vitorino, R., Hojjat, S.P., Ma, A.Y., Zhang, L., Lee, L., Carroll, T.J., Cantrell, C.G., Figley, C.R., Aviv, R.I., 2017. Spatial correlation of pathology and perfusion changes within the cortex and white matter in multiple sclerosis. Am. J. Neuroradiol. 39 (1), 91–96.
Mulligan, S.J., MacVicar, B.A., 2004. Calcium transients in astrocyte endfeet cause cerebrovascular constrictions. Nature 431 (7005), 195–200.
Nagy, Z., Westerberg, H., Klingberg, T., 2004. Maturation of white matter is associated with the development of cognitive functions during childhood. J. Cognit. Neurosci. 16 (7), 1227–1233.
Ogawa, S., Lee, T., Kay, A., Tank, D., 1990. Brain magnetic resonance imaging with contrast dependent on blood oxygenation. Proc. Natl. Acad. Sci. U. S. A. 9868–9872.
Ogawa, S., Tank, D.W., Menon, R., Ellermann, J.M., Kim, S.G., Merkle, H., Ugurbil, K., 1992. Intrinsic signal changes accompanying sensory stimulation: functional brain mapping with magnetic resonance imaging. Proc. Natl. Acad. Sci. U. S. A. 89 (13), 5951–5955.
Pantano, P., Mainero, C., Lenzi, D., Caramia, F., Iannetti, G.D., Piattella, M.C., Pestalozza, I., Di Legge, S., Bozzao, L., Pozzilli, C., 2005. A longitudinal fMRI study on motor activity in patients with multiple sclerosis. Brain 128 (9), 2146–2153.
Pasley, B.N., Inglis, B.A., Freeman, R.D., 2007. Analysis of oxygen metabolism implies a neural origin for the negative BOLD response in human visual cortex. Neuroimage 36 (2), 269–276.
Petzold, G.C., Murthy, V.N., 2011. Role of astrocytes in neurovascular coupling. Neuron 71 (5), 782–797.
Pirko, I., Lucchinetti, C.F., Sriram, S., Bakshi, R., 2007. Gray matter involvement in multiple sclerosis. Neurology 68 (9), 634–642.
Rae, C.L., Correia, M.M., Altena, E., Hughes, L.E., Barker, R.A., Rowe, J.B., 2012. White matter pathology in Parkinson's disease: the effect of imaging protocol differences and relevance to executive function. Neuroimage 62 (3), 1675–1684.
Ramsay, J.O., 2006. Functional Data Analysis. John Wiley & Sons, Inc.
Rashid, W., Parkes, L.M., Ingle, G.T., Chard, D.T., Toosy, A.T., Altmann, D.R., Symms, M.R., Tofts, P.S., Thompson, A.J., Miller, D.H., 2004. Abnormalities of cerebral perfusion in multiple sclerosis. J. Neurol. Neurosurg. Psychiatr. 75 (9), 1288–1293.
Restom, K., Bangen, K.J., Bondi, M.W., Perthen, J.E., Liu, T.T., 2007. Cerebral blood flow and BOLD responses to a memory encoding task: a comparison between healthy young and elderly adults. Neuroimage 37 (2), 430–439.
Rinholm, J.E., Bergersen, L.H., 2012. The wrap that feeds neurons. Nature 487 (7408), 435.
Rocca, M.A., Falini, A., Colombo, B., Scotti, G., Comi, G., Filippi, M., 2002. Adaptive functional changes in the cerebral cortex of patients with nondisabling multiple sclerosis correlate with the extent of brain structural damage. Ann. Neurol. 51 (3), 330–339.
Rossi, D.J., 2006. Another BOLD role for astrocytes: coupling blood flow to neural activity. Nat. Neurosci. 9, 159–160.
Rypma, B., D'Esposito, M., 1999. The roles of prefrontal brain regions in components of working memory: effects of memory load and individual differences. Proc. Natl. Acad. Sci. U. S. A. 96 (11), 6558–6563.
Rypma, B., D'Esposito, M., 2001. Age-related changes in brain–behaviour relationships: evidence from event-related functional MRI studies. Eur. J. Cognit. Psychol. 13 (1–2), 235–256.
Rypma, B., Prabhakaran, V., 2009. When less is more and when more is more: the mediating roles of capacity and speed in brain-behavior efficiency. Intelligence 37 (2), 207–222.
Rypma, B., Berger, J.S., Prabhakaran, V., Bly, B.M., Kimberg, D.Y., Biswal, B.B., D'Esposito, M., 2006. Neural correlates of cognitive efficiency. Neuroimage 33 (3), 969–979, 2006 Nov 15.
Rypma, B., Eldreth, D.A., Rebbechi, D., 2007. Age-related differences in activation-performance relations in delayed-response tasks: a multiple component analysis. Cortex 43 (1), 65–76.
Rypma, B., Prabhakaran, V., Desmond, J.E., Glover, G.H., Gabrieli, J.D., 1999. Load-dependent roles of frontal brain regions in the maintenance of working memory. Neuroimage 9 (2), 216–226.
Salat, D.H., Kaye, J.A., Janowsky, J.S., 1999. Prefrontal gray and white matter volumes in healthy aging and Alzheimer disease. Arch. Neurol. 56 (3), 338–344.
Salthouse, T.A., 1992. Influence of processing speed on adult age differences in working memory. Acta Psychol. 79 (2), 155–170.
Salthouse, T., 1996. The processing-speed theory of adult age differences in cognition. Psychol. Rev. 403–428.
Stefanovic, B., Warnking, J.M., Pike, G.B., 2004. Hemodynamic and metabolic responses to neuronal inhibition. Neuroimage 22 (2), 771–778.
Strober, L.B., Rao, S.M., Lee, J.C., Fischer, E., Rudick, R., 2014. Cognitive impairment in multiple sclerosis: an 18 year follow-up study. Mult. Scler. Relat. Disord. 3 (4), 473–481.
Su, K.G., Banker, G., Bourdette, D., Forte, M., 2009. Axonal degeneration in multiple sclerosis: the mitochondrial hypothesis. Curr. Neurol. Neurosci. Rep. 9 (5), 411–417.
Sun, X., Tanaka, M., KoNDo, S., Okamoto, K., Hirai, S., 1998. Clinical significance of reduced cerebral metabolism in multiple sclerosis: a combined PET and MRI study. Ann. Nucl. Med. 12 (2), 89–94.
Swank, R.L., Roth, J.G., Woody Jr., D.C., 1983. Cerebral blood flow and red cell delivery in normal subjects and in multiple sclerosis. Neurol. Res. 5 (1), 37–59.
Takano, T., Tian, G.F., Peng, W., Lou, N., Libionka, W., Han, X., Nedergaard, M., 2006. Astrocyte-mediated control of cerebral blood flow. Nat. Neurosci. 9 (2), 260–267.
Tombaugh, T.N., Rees, L., McIntyre, N., 1998. Normative Data for the Trail Making Test. A Compendium of Neuropsychological Tests: Administration. Oxford University Press, New York.
Trapp, B.D., Nave, K.A., 2008. Multiple Sclerosis: an immune or neurodegenerative disorder? Annu. Rev. Neurosci. 31, 247–269.
Trapp, B.D., Stys, P.K., 2009. Virtual hypoxia and chronic necrosis of demyelinated axons in multiple sclerosis. Lancet Neurol. 8 (3), 280–291.
Tsvetanov, K.A., Henson, R.N., Tyler, L.K., Davis, S.W., Shafto, M.A., Taylor, J.R., Williams, N., Cam-CAN, Rowe, J.B., 2015. The effect of ageing on fMRI: correction for the confounding effects of vascular reactivity evaluated by joint fMRI and MEG in 335 adults. Hum. Brain Mapp. 36 (6), 2248–2269.
Turner, M.P., Hubbard, N.A., Himes, L.M., Faghihahmadabadi, S., Hutchison, J.L., Bennett, I.J., Motes, M.A., Haley, R.W., Rypma, B., 2016. Cognitive slowing in Gulf

war illness predicts executive network hyperconnectivity: study in a population-representative sample. Neuroimage Clin. 12, 535–541.
Varga, A.W., Johnson, G., Babb, J.S., Herbert, J., Grossman, R.I., Inglese, M., 2009. White matter hemodynamic abnormalities precede sub-cortical gray matter changes in multiple sclerosis. J. Neurol. Sci. 282 (1), 28–33.
Vercellino, M., Masera, S., Lorenzatti, M., Condello, C., Merola, A., Mattioda, A., Tribolo, A., Capello, E., Mancardi, G.L., Mutani, R., Giordana, M.T., Cavalla, P., 2009. Demyelination, inflammation, and neurodegeneration in multiple sclerosis deep gray matter. J. Neuropathol. Exp. Neurol. 68 (5), 489–502.
Vernon, P.A., 1983. Speed of information processing and general intelligence. Intelligence 7 (1), 53–70.
Ward, B.D., 2000. Deconvolution analysis of fMRI time series data [software manual]. (1998/2006). Retrieved from: https://afni.nimh.nih.gov/pub/dist/doc/manual/Deconvolvem.pdf.
Wechsler, D., 1997. WAIS-III: Administration and Scoring Manual: Wechsler Adult Intelligence Scale. Psychological Corporation, San Antonio, TX.
Wegner, C., Filippi, M., Korteweg, T., Beckmann, C., Ciccarelli, O., De Stefano, N., Enzinger, C., Fazekas, F., Agosta, F., Gass, A., Hirsch, J., Johansen-Berg, H., Kappos, L., Barkhof, F., Polman, C., Mancini, L., Manfredonia, F., Marino, S., Miller, D.H., Montalban, X., Palace, J., Rocca, M., Ropele, S., Rovira, A., Smith, S., Thompson, A., Thornton, J., Yousry, T., Matthews, P.M., 2008. Relating functional changes during hand movement to clinical parameters in patients with multiple sclerosis in a multi-centre fMRI study. Eur. J. Neurol. 15 (2), 113–122.
White, A.T., Lee, J.N., Light, A.R., Light, K.C., 2009. Brain activation in multiple sclerosis: a BOLD fMRI study of the effects of fatiguing hand exercise. Mult. Scler. J. 15 (5), 580–586.
Wink, A.M., Hoogduin, H., Roerdink, J.B., 2008. Data-driven haemodynamic response function extraction using Fourier-wavelet regularised deconvolution. BMC Med. Imag. 8 (1), 7.
Xu, F., Liu, P., Pascual, J.M., Xiao, G., Lu, H., 2012. Effect of hypoxia and hyperoxia on cerebral blood flow, blood oxygenation, and oxidative metabolism. J. Cerebr. Blood Flow Metabol. 32, 1909–1918.
Zhang, H., Avants, B.B., Yushkevich, P.A., Woo, J.H., Wang, S., McCluskey, L.F., Elman, L.B., Melhem, E.R., Gee, J.C., 2007. High-dimensional spatial normalization of diffusion tensor images improves the detection of white matter differences: an example study using amyotrophic lateral sclerosis. IEEE Trans. Med. Imag. 26 (11), 1585–1597.
Zou, P., Helton, K.J., Smeltzer, M., Li, C.S., Conklin, H.M., Gajjar, A., Wang, W.C., Ware, R.E., Ogg, R.J., 2011. Hemodynamic responses to visual stimulation in children with sickle cell anemia. Brain Imag. Behav. 5 (4), 295–306.